Antagonistic Control of Disease Resistance Protein Stability in the Plant Immune System

Ben F. Holt III,[1]* Youssef Belkhadir,[1]* Jeffery L. Dangl[1,2,3,4]†

Pathogen recognition by the plant immune system is governed by structurally related, polymorphic products of disease resistance (*R*) genes. RAR1 and/or SGT1b mediate the function of many R proteins. RAR1 controls preactivation R protein accumulation by an unknown mechanism. We demonstrate that *Arabidopsis* SGT1b has two distinct, genetically separable functions in the plant immune system: SGT1b antagonizes RAR1 to negatively regulate R protein accumulation before infection, and SGT1b has a RAR1-independent function that regulates programmed cell death during infection. The balanced activities of RAR1 and SGT1, in concert with cytosolic HSP90, modulate preactivation R protein accumulation and signaling competence.

Specificity in the *Arabidopsis* immune system relies on ~125 polymorphic disease resistance (*R*) genes, many of which encode NB-LRR proteins containing nucleotide binding sites and leucine-rich repeats. NB-LRR proteins "recognize" pathogen proteins that can contribute to pathogen virulence in the absence of host recognition. When recognized by the plant, these are termed avirulence (Avr) proteins. Pathogens from various kingdoms trigger similar NB-LRR-mediated defense responses. Conserved plant proteins control NB-LRR signaling (*1*, *2*). These include *RAR1*, *SGT1*, and cytosolic HSP90, each identified by recessive mutations and/or gene silencing in barley, *Arabidopsis*, potato, tobacco, and tomato (*3*–*8*).

RAR1 plays a generic role in maintaining preactivation NB-LRR protein levels (*9*–*11*) (see below). However, *rar1* mutants suppress the resistance function of only a subset of

[1]Department of Biology, [2]Curriculum in Genetics, [3]Department of Microbiology and Immunology, [4]Carolina Center for Genome Sciences, University of North Carolina, Chapel Hill, NC 27599, USA.

*These authors contributed equally to this work.
†To whom correspondence should be addressed. Department of Biology, 108 Coker Hall, University of North Carolina, CB# 3280, Chapel Hill, NC 27599–3280, USA. E-mail: dangl@email.unc.edu

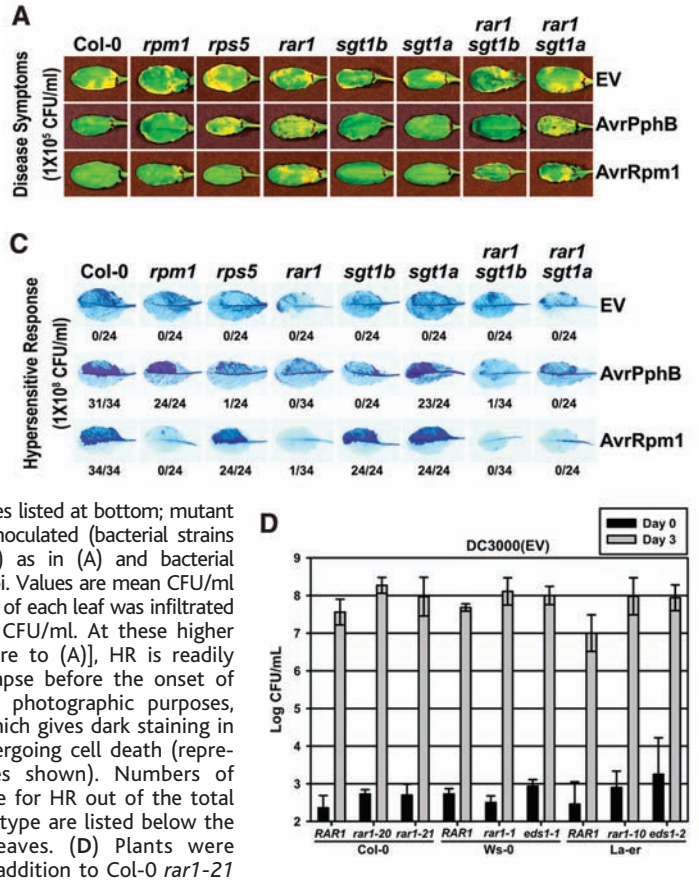

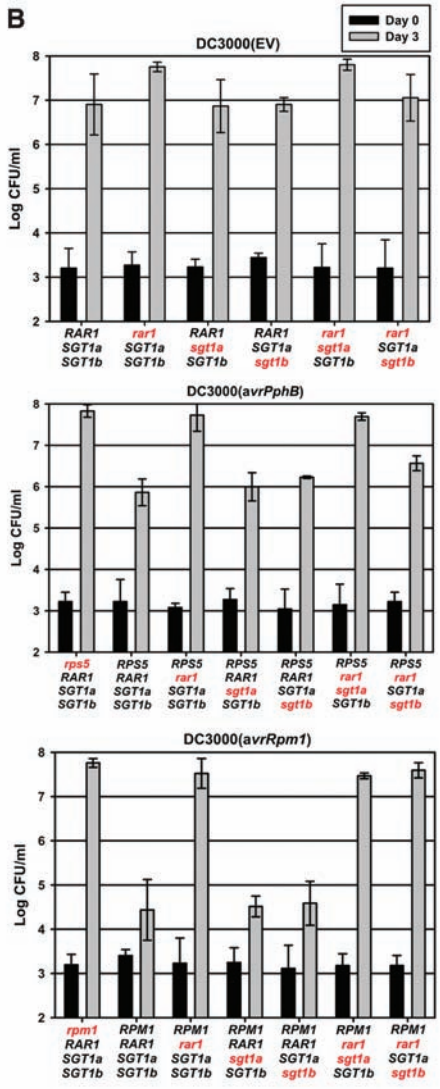

Fig. 1. *SGT1b* antagonizes *RAR1* to control *RPS5*-mediated disease resistance. (**A**) *Pseudomonas syringae* pv. *tomato* (*Pto* DC3000) carrying empty vector (EV) or expressing *avrPphB* (to trigger RPS5) or *avrRpm1* (to trigger RPM1) was infiltrated into leaves at ~1 × 10^5 colony forming units (CFU)/ml. Photos of disease symptoms were taken 5 days postinoculation (dpi). Plant lines, alternative alleles tested, extended protocols, and genotyping are described in (*30*). (**B**) Plants (genotypes listed at bottom; mutant loci in red) were hand inoculated (bacterial strains listed above each panel) as in (A) and bacterial growth was assessed 3 dpi. Values are mean CFU/ml ± 2 SE. (**C**) The upper half of each leaf was infiltrated as in (A) with 1 × 10^8 CFU/ml. At these higher inoculum levels [compare to (A)], HR is readily observed as tissue collapse before the onset of disease symptoms. For photographic purposes, we used trypan blue, which gives dark staining in regions of the leaf undergoing cell death (representative trypan leaves shown). Numbers of leaves scored as positive for HR out of the total examined for each genotype are listed below the trypan blue–stained leaves. (**D**) Plants were inoculated as in (A). In addition to Col-0 *rar1-21* [*rar1* allele used in (A)], we tested additional *Arabidopsis* ecotypes and *rar1* alleles. As controls for mutant lines with reduced basal resistance, we inoculated enhanced disease susceptibility (*eds1*) mutants.

NB-LRR proteins. A "threshold model" can explain the discrepancy between genetic requirements for RAR1 and its apparent biochemical function (*11*). Thus, *RAR1*-"independent" NB-LRR proteins accumulate to relatively high steady-state levels and remain above a threshold required for efficient defense activation even when destabilized in a *rar1* background. In contrast, *RAR1*-"dependent" NB-LRR proteins accumulate to relatively low levels that fall below a critical threshold in *rar1* mutants. Consistent with the semidominant nature of many *R*-mediated responses, the threshold model predicts that NB-LRR proteins are quantitative, response-limiting regulators. Cytosolic HSP90 is an additional determinant of steady-state NB-LRR protein accumulation (*12*). RAR1 likely collaborates with cytosolic HSP90 as a co-chaperone maintaining signal-competent NB-LRR proteins (*13*–*16*).

In yeast, SGT1 functions in kinetochore and SCF ubiquitin-ligase assembly (*17*–*19*). *Arabidopsis* has two SGT1 paralogs, *SGT1a* and *SGT1b* (78% amino acid identity), but only *sgt1b* mutations suppress NB-LRR function (*7*, *8*, *20*). RAR1, SGT1, and HSP90 interact in vivo, and RAR1 and SGT1 each interact with subunits of the COP9 signalosome, a likely proteasome lid complex (*5*, *14*, *20*). Further, SGT1 interacts with SCF ubiquitin ligase components, provoking speculation that SGT1 mediates the degradation of negative regulators of plant immune function (*20*). Concomitant losses of RAR1 and SGT1b additively impair function of the *Arabidopsis* NB-LRR protein RPP5 (*7*), suggesting separable activities for these two genes. Accordingly, we define a RAR1-independent SGT1b function in programmed cell death. Unexpectedly, however, our data also demonstrate that SGT1b can negatively regulate NB-LRR protein accumulation, and that this activity is antagonized by both RAR1 and HSP90.

The *Arabidopsis* NB-LRR proteins RPM1, RPS2, and RPS5 confer resistance to *Pseudomonas syringae*. Each is impaired in *rar1* (*10*, *20*, *21*), but unaffected in *sgt1a* or *sgt1b* (*7*, *22*) (Fig. 1, A and B). Unexpectedly, *RPS5* function, but not *RPM1* or *RPS2* function, was recovered in *rar1 sgt1b* (Fig. 1, A and B; *RPS2* data not shown). None of the *rar1* mutant phenotypes were recovered in *rar1 sgt1a*. Therefore, *SGT1b* mediates the loss of *RPS5* function in *rar1*, whereas *SGT1a* and *SGT1b* may act redundantly in this process for *RPM1* and *RPS2* (*6*).

NB-LRR activation often triggers a rapid localized programmed cell death, called the hypersensitive response (HR) (*23*). The HR likely limits the growth of biotrophic fungi and oomycetes (*4*, *21*, *24*, *25*), although its role in resistance to bacterial pathogens is unclear. *RAR1* is required for *RPS5*-, *RPM1*-, and *RPS2*-mediated HR (*10*). Of these, only the *RPS5*-mediated HR additionally required *SGT1b* (Fig. 1C; fig. S1A). Neither *RPS5*-, *RPM1*-, nor *RPS2*-dependent HR were restored in *rar1 sgt1b*. Using the oomycete parasite *Peronospora parasitica*, we extended these findings to two additional NB-LRR functions (*RPP4* and *RPP31*; fig. S1, B to E). Thus, *SGT1b* can control the HR in a *RAR1*-independent manner. Further, NB-LRR–mediated disease resistance and HR are genetically separable.

Notably, *rar1* mutations in different genetic backgrounds allowed enhanced growth of the virulent bacterial strain *P. syringae* (*Pto*) DC3000 (Fig. 1, B and D). These data demonstrate a role for *RAR1* in basal resistance, an ostensibly *R*-independent response that limits pathogen spread in susceptible plants (*1*). This *rar1* phenotype is also suppressed in *rar1 sgt1b*, but not *rar1 sgt1a* (Fig. 1D). Therefore, *SGT1b* also antagonizes *RAR1* in the control of basal resistance. Given that the only known function for *RAR1* is to promote NB-LRR protein accumulation, then NB-LRR proteins also are very likely to function in basal resistance.

Requirements for *RAR1* and *SGT1b* have been defined for NB-LRR genes that confer resistance to different isolates of the oomycete parasite *Peronospora parasitica* (*Pp*) (table S1). *RPP8* was weakly impaired by *rar1*, as indicated by low levels of asexual parasite sporulation (Fig. 2, A and B). We bred isogenic plants hemizygous for an *RPP8* transgene (*RPP8/-*) in each mutant background to determine whether the small phenotypic effect of *rar1* might depend on *RPP8* dosage. *RPP8/− rar1* plants exhibited increased susceptibility as compared to homozygous controls, supporting the threshold model (*11*). *RPP8/− rar1 sgt1b* plants were completely resistant, indicating that *SGT1b* mediates susceptibility in *RPP8/− rar1*. As with *RPP4*, *RPP31*, and *RPS5*, these data are inconsistent with the hypothesis that *RAR1* and *SGT1* act additively in all NB-LRR–mediated disease resistance responses.

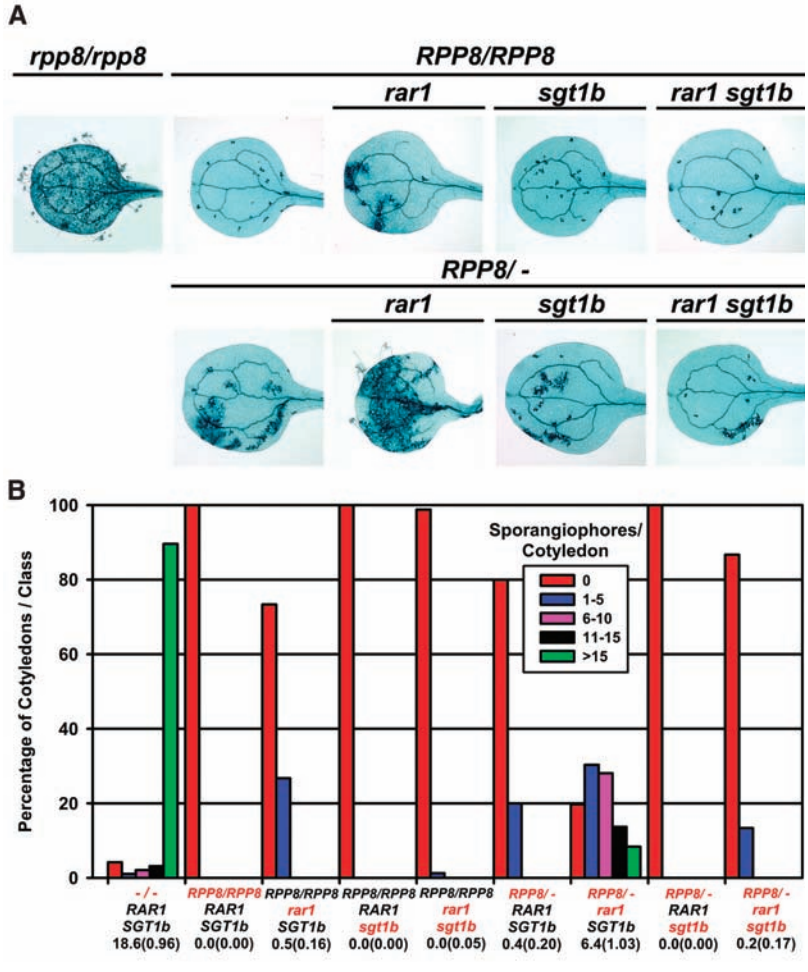

Fig. 2. SGT1b antagonism of RAR1 is generalizable to several NB-LRR resistance specificities. (**A**) Seven- to 10-day-old cotyledons of *rpp8* plants expressing a stable *RPP8* transgene were inoculated with the asexual spores of *Peronospora parasitica* (*Pp*) isolate Emco5 (*40*). Representative, trypan blue–stained leaves are shown to illustrate cell death and *Pp* structures (hyphae, asexual sporangiophores). (**B**) Asexual sporangiophores were quantified 7 dpi on at least 50 cotyledons for each of the indicated genetic backgrounds. The numbers below each tested genotype (key genotypes shown in red) represent mean sporangiophores/cotyledon (± 2 SE).

To further investigate the recovery of *RPS5*-mediated disease resistance in *rar1 sgt1b*, we constructed isogenic lines expressing hemagglutinin (HA) epitope-tagged RPS5 driven by the native promoter in the La-er ecotype (an *rps5* null) (*26*). RPS5:HA accumulated exclusively in the microsomal fraction of wild-type, *rar1*, and *sgt1b*, and its accumulation was greatly diminished in *rar1* (Fig. 3A). These results are similar to previous observations for RPM1 and RPS2 (*9*, *10*, *27*, *28*).

Unregulated NB-LRR expression can be lethal, suggesting that R protein accumulation must be fine tuned to provide rapid responses to infection while minimizing aberrant signaling. Dose dependence of *MLA1* (*11*) and *RPP8* (Fig. 2) suggested that NB-LRR–mediated responses should be proportional to their steady-state protein accumulation levels. To test this hypothesis, we used the inherent variability of RPS5:HA accumulation in 10 independent transgenic lines. After *Pto* DC3000 inoculation, random *RPS5:HA rps5* transgenic plants were ordered according to HR timing, from no HR to rapid HR. Protein samples from this phenotypically ordered set of plants demonstrated that increasing RPS5:HA protein levels correlated with faster HR (Fig. 3B). Thus, the levels of RPS5, and presumably other NB-LRR proteins, can be rate limiting for response rapidity. These data further support the RAR1-mediated threshold model for NB-LRR function (*11*).

We quantified RPS5:HA accumulation in individual, first-generation transgenic plants of each relevant genotype (Fig. 3C). RPS5:HA accumulated to readily detectable, equivalent mean levels in La-er wild type and *sgt1b*, but to only 13% of wild-type levels in *rar1*. RPS5:HA accumulation was restored to ~60% of wild-type levels in *rar1 sgt1b*. By contrast, and as expected from the lack of RPM1 functional recovery (Fig. 1B), RPM1:Myc did not reaccumulate in *rar1 sgt1b* (Fig. 3D).

We created genetic controls to confirm the antagonistic roles of RAR1 and SGT1b in RPS5 accumulation. A *rar1/rar1* transgenic parental line expressing low, but measurable RPS5:HA was used to generate *RPS5:HA*

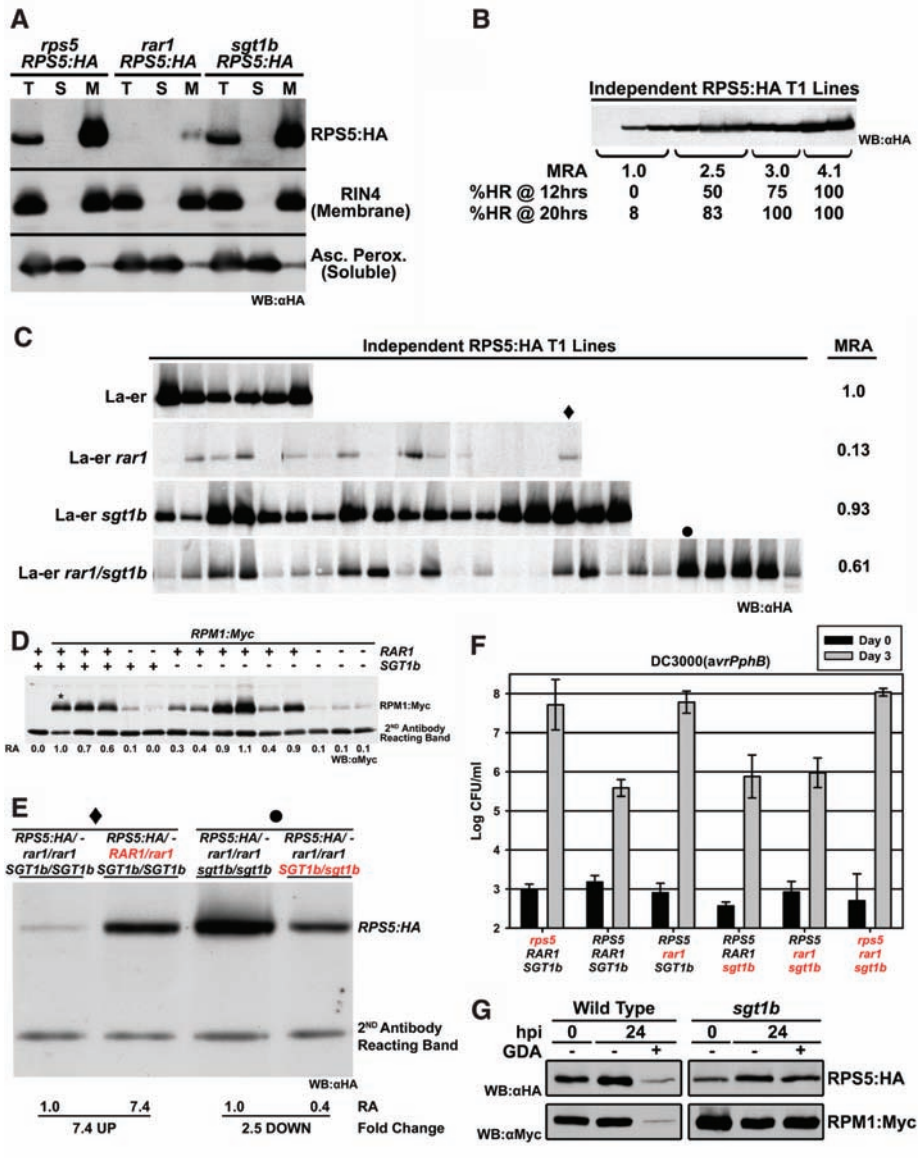

Fig. 3. RAR1 and SGT1 act antagonistically to control RPS5 protein accumulation. (**A**) Tissue samples for protein blot analysis were taken from independent, F_1 plants transformed with an HA epitope–tagged *RPS5* transgene [*RPS5:HA* (*30*)]. Protein was separated into total (T), soluble (S), and membrane (M) fractions (*28*). Ascorbate peroxidase and RIN4 antibodies were used as controls for the cytoplasmic and membrane fractions, respectively (*41*, *42*). Equal loading for all protein samples in Fig. 3 was ensured by protein quantification before loading and Ponceau Red staining of nitrocellulose membranes after transfer. (**B**) Total protein extracts were isolated from 10 independent, F_1 Col-0 *rps5* mutants transformed with the *RPS5:HA* transgene. Before protein blot analysis, four leaves per plant were visually scored for HR (as in Fig. 1C) at 12 and 20 hours (%HR@12 or 20 hrs). Mean relative RPS5:HA protein accumulation (MRA) levels were quantified using ImageJ (version 1.31) (*43*). All values were transformed such that the weakest RPS5:HA-expressing plants (first three lanes on blot) were equalized to MRA = 1.0. (**C**) La-er (*rps5*) ecotype plants and the *rar1*, *sgt1b*, and *rar1 sgt1b* mutants [also in La-er (*30*)] were transformed with the *RPS5:HA* transgene. Individual, F_1 transformants were selected in each genetic background, and RPS5:HA protein accumulation was visualized by protein blot. MRA values were transformed such that pooled values from the wild-type La-er ecotype was set to 1.0. Symbols above *rar1* and *rar1 sgt1b* lanes are explained in (E). (**D**) A stable RPM1:Myc transgenic line (*28*) was crossed to the *rar1 sgt1b* mutant. Indicated genotypes were selected by polymerase chain reaction from the F_2 population and examined by protein blot analysis as in (C). The lane designated with an asterisk (*) represents the parental RPM1:Myc line. (**E**) A La-er *RPS5:HA/- rar1/rar1* transformant [male; (♦) in (C)] was crossed to either La-er *rar1/rar1* or La-er *RAR1/RAR1* (females in each cross). Similarly, a La-er *RPS5:HA/- rar1/rar1 sgt1b/sgt1b* transformant [male; (●) in (C)] was crossed to either La-er *rar1/rar1 sgt1b/sgt1b* or La-er *rar1/rar1 SGT1b/SGT1b* (females). The resulting genotypes are shown above each lane. The first lane of each pair recapitulates the original parental genotype, and the second represents altered gene dosages of either RAR1 or SGT1b (red text). The secondary antibody reacting band further demonstrates equal loading. Relative accumulation (RA) levels were transformed such that the parental lane in each comparison equals 1.0. (**F**) Stable, nonsegregating *rps5 rar1 sgt1b* triple-mutant plants were isolated and tested for disease resistance as in Fig. 1B. (**G**) Leaves were infiltrated with either dimethyl sulfoxide (DMSO) alone or 10 μM geldanamycin (GDA; A.G. Scientific, San Diego, CA) dissolved in DMSO (*30*). Samples were collected for protein blot analysis 24 hours after inoculation (similar results were seen at 18 hours). GDA did not alter RPS2:HA accumulation (data not shown) (*30*).

RAR1/rar1 and sibling control F_1 plants (Fig. 3E, first two columns). RPS5:HA accumulation was restored more than sevenfold in the *RAR1/rar1* heterozygote. Similarly, a *rar1 sgt1b* transgenic parent that accumulated high levels of RPS5:HA was used to generate *RPS5:HA rar1/rar1 SGT1b/sgt1b* and sibling control F_1 plants (Fig. 3E, third and fourth columns). The presence of a single copy of wild-type *SGT1b* resulted in 2.5 fold less RPS5:HA than in sibling controls. Importantly, disease resistance observed in *RPS5 rar1 sgt1b* (Fig. 1, A and B) was lost in an *rps5 rar1 sgt1b* triple mutant (Fig. 3F), demonstrating a direct link between restoration of *RPS5* function and RPS5 protein levels. Collectively, these data demonstrate that RAR1 is a positive regulator, and SGT1b a negative regulator, of RPS5 accumulation. We envision that the recovery we observed for other NB-LRR functions in *rar1 sgt1b* (Fig. 2 and fig. S1, B to E) follows the same mechanism.

Reduction of cytosolic HSP90 function negatively affects steady-state accumulation of NB-LRR proteins (*12*, *14*). We used the HSP90-specific inhibitor geldanamycin (GDA) (*29*) to examine RPS5:HA and RPM1:Myc protein accumulation in wild-type and *sgt1b* plants. GDA infiltration into wild-type leaves typically resulted in reduced RPS5:HA and RPM1:Myc protein accumulation, but did not eliminate disease resistance function (Fig. 3G) (*30*). GDA did not affect accumulation of either NB-LRR protein in *sgt1b*. Thus, elimination of RAR1 or inhibition of HSP90 activity is sufficient to lower NB-LRR protein accumulation through an unknown mechanism. In both cases, SGT1b can mediate this outcome. Notably, RPM1:Myc destabilization mediated by GDA is SGT1b dependent, whereas its destabilization in *rar1* is not. This contrasts with RPS5:HA, suggesting that antagonism between RAR1-HSP90 and SGT1b is fine tuned for different NB-LRR proteins.

Our findings challenge suggestions of signaling functions for RAR1 and SGT1b in NB-LRR–mediated disease resistance. Restoration of *RPS5*-, *RPP4*-, *RPP8*-, and *RPP31*-mediated functions in *rar1 sgt1b* prove that RAR1 and SGT1b are not required for disease resistance signaling per se. Additionally, we show that SGT1b has a RAR1-independent function as a positive regulator of *RPP4*-, *RPP31*-, and *RPS5*-mediated HR. A general role for SGT1b in HR is now well established (*6*, *31*), and we speculate that an efficient HR requires SGT1b-dependent elimination of an unidentified negative regulator. This SGT1b function would be particularly relevant in cases where HR plays a key role in limiting pathogen spread, explaining why some NB-LRR proteins exhibit additive requirements for RAR1 and SGT1b. In such cases, the lack of NB-LRR accumulation in *rar1 sgt1b* coupled to an inefficient HR would result in enhanced pathogen growth.

RAR1 and HSP90 are positive regulators of NB-LRR protein steady-state accumulation [(*9*–*12*, *14*) and this work]. As such, RAR1 and HSP90 may determine whether NB-LRR proteins are functional in disease resistance or marked for degradation. Cytosolic HSP90 transiently binds nonnative "client" proteins to assist in proper folding (*32*, *33*). Active folding of HSP90 client proteins is regulated by cycles of adenosine 5′-triphosphate (ATP) binding and hydrolysis that are, in turn, modulated by co-chaperones. In addition to modulating ATP hydrolysis, co-chaperones also guide HSP90 client specificity. Therefore, HSP90 apparently processes and/or maintains NB-LRR proteins to a signal-competent conformational state, with RAR1 acting as a co-chaperone.

Yeast SGT1 transiently links HSP90 to the inner kinetochore complex (CBF3), balancing CBF3 assembly and turnover (*34*). Specific mutations that "trap" SGT1 in CBF3 complexes result in reduced CBF3 accumulation. This is consistent with our finding that elimination of SGT1b can reduce NB-LRR turnover. We speculate that RAR1 defines a regulatory checkpoint protecting HSP90-associated NB-LRR proteins from SGT1b-mediated degradation. In *rar1* mutants, this degradation pathway becomes the default, perhaps through direct interaction of HSP90-associated NB-LRR proteins with an SCF-bound SGT1 (*11*, *35*, *36*).

Coupling of folding and degradation fates has previously been demonstrated for the HSP90 clients glucocorticoid hormone receptor (GR) and cystic fibrosis transmembrane conductance regulator (CFTR) (*37*, *38*). GR or CFTR, in complex with HSP70/HSP90, are degraded when these complexes associate with CHIP (carboxy-terminus of HSP70 interacting protein), a member of the U-box family of ubiquitin ligases. Mutations in CHIP that eliminate ubiquitin ligase function dominantly interfere with ubiquitination and subsequent GR/CFTR degradation. Like SGT1, CHIP has several tetratricopeptide repeats (TPRs) that are required for HSP70/HSP90 association (*15*, *19*, *37*). Therefore, like CHIP, SGT1-SCF complexes might couple NB-LRR proteins to the cellular degradation machinery (*39*). It remains unclear whether changes in NB-LRR accumulation are due to proteasome-dependent degradation or an alternative protein turnover mechanism such as endocytosis. Nevertheless, we anticipate that our genetic results will inform subsequent biochemical experiments.

References and Notes

1. J. L. Dangl, J. D. G. Jones, *Nature* **411**, 826 (2001).
2. Y. Belkhadir, R. Subramaniam, J. L. Dangl, *Curr. Opin. Plant Biol.* **7**, 391 (2004).
3. Y. Liu, M. Schiff, R. Marathe, S. P. Dinesh-Kumar, *Plant J.* **30**, 415 (2002).
4. K. Shirasu *et al.*, *Cell* **99**, 355 (1999).
5. Y. Liu, M. Schiff, G. Serino, X. W. Deng, S. P. Dinesh-Kumar, *Plant Cell* **14**, 1483 (2002).
6. J. R. Peart *et al.*, *Proc. Natl. Acad. Sci. U.S.A.* **99**, 10865 (2002).
7. M. J. Austin *et al.*, *Science* **295**, 2077 (2002).
8. M. Tör *et al.*, *Plant Cell* **14**, 993 (2002).
9. Y. Belkhadir, Z. Nimchuk, D. A. Hubert, D. Mackey, J. L. Dangl, *Plant Cell* **16**, 2822 (2004).
10. P. Tornero *et al.*, *Plant Cell* **14**, 1005 (2002).
11. S. Bieri *et al.*, *Plant Cell* **16**, 3480 (2004).
12. R. Lu *et al.*, *EMBO J.* **22**, 5690 (2003).
13. Y. Liu, T. Burch-Smith, M. Schiff, S. Feng, S. P. Dinesh-Kumar, *J. Biol. Chem.* **279**, 2101 (2004).
14. D. A. Hubert *et al.*, *EMBO J.* **22**, 5679 (2003).
15. A. Takahashi, C. Casais, K. Ichimura, K. Shirasu, *Proc. Natl. Acad. Sci. U.S.A.* **100**, 11777 (2003).
16. K. Shirasu, P. Schulze-Lefert, *Trends Plant Sci.* **8**, 252 (2003).
17. K. Kitagawa, D. Skowyra, S. J. Elledge, J. W. Harper, P. Hieter, *Mol. Cell* **4**, 21 (1999).
18. P. Steensgaard *et al.*, *EMBO Rep.* **5**, 626 (2004).
19. P. K. Bansal, R. Abdulle, K. Kitagawa, *Mol. Cell. Biol.* **24**, 8069 (2004).
20. C. Azevedo *et al.*, *Science* **295**, 2073 (2002).
21. P. R. Muskett *et al.*, *Plant Cell* **14**, 979 (2002).
22. R. F. Warren, P. M. Merritt, E. Holub, R. W. Innes, *Genetics* **152**, 401 (1999).
23. J. L. Dangl, R. A. Dietrich, M. H. Richberg, *Plant Cell* **8**, 1793 (1996).
24. L. Belbahri *et al.*, *Plant J.* **28**, 419 (2001).
25. A. Freialdenhoven *et al.*, *Plant Cell* **6**, 983 (1994).
26. M. T. Simonich, R. W. Innes, *Mol. Plant Microbe Interact.* **8**, 637 (1995).
27. M. J. Axtell, B. J. Staskawicz, *Cell* **112**, 369 (2003).
28. D. C. Boyes, J. Nam, J. L. Dangl, *Proc. Natl. Acad. Sci. U.S.A.* **95**, 15849 (1998).
29. S. M. Roe *et al.*, *J. Med. Chem.* **42**, 260 (1999).
30. Materials and methods are available as supporting material on *Science* Online.
31. Y. Zhang, S. Dorey, M. Swiderski, J. D. Jones, *Plant J.* **40**, 213 (2004).
32. J. C. Young, I. Moarefi, F. U. Hartl, *J. Cell Biol.* **154**, 267 (2001).
33. T. A. Sangster, C. Queitsch, *Curr. Opin. Plant Biol.* **8**, 86 (2005).
34. L. B. Lingelbach, K. B. Kaplan, *Mol. Cell. Biol.* **24**, 8938 (2004).
35. C. Dubacq, R. Guerois, R. Courbeyrette, K. Kitagawa, C. Mann, *Eukaryot. Cell* **1**, 568 (2002).
36. Yeast SGT1 interacts with the LRR of Cyr1p/Cdc35p adenylyl cyclase, and barley SGT1 interacts with the LRR of barley NB-LRR protein MLA1. However, full-length MLA1 does not interact with SGT1, consistent with the suggestion that NB-LRR conformation is regulated by intramolecular interactions that differ between pre- and postinfection states. We found that the LRR domains of RPM1, RPS2, and RPS5 did not interact with either SGT1a or SGT1b in yeast two-hybrid experiments, although we were able to reproduce the MLA1-SGT1 interaction. We also found no obvious proteasome function in RPS5 degradation (*30*).
37. P. Connell *et al.*, *Nat. Cell Biol.* **3**, 93 (2001).
38. G. C. Meacham, C. Patterson, W. Zhang, J. M. Younger, D. M. Cyr, *Nat. Cell Biol.* **3**, 100 (2001).
39. J. Höhfeld, D. M. Cyr, C. Patterson, *EMBO Rep.* **2**, 885 (2001).
40. J. M. McDowell *et al.*, *Plant Cell* **10**, 1861 (1998).
41. H. M. Jespersen, I. V. Kjaersgard, L. Ostergaard, K. G. Welinder, *Biochem. J.* **326**, 305 (1997).
42. D. Mackey, B. F. Holt III, A. Wiig, J. L. Dangl, *Cell* **108**, 743 (2002).
43. http://rsb.info.nih.gov/ij/

44. Supported by NSF *Arabidopsis* 2010 grant (IBN-0114795). We thank D. Hubert, J. Chang, J. McDowell, E. Holub, and J. Jones for critical evaluations of the manuscript. We also thank P. Muskett and J. Parker for providing La-er *rar1-10* and *sgt1b-1* seeds and W. Gray for *sgt1b*^{eta3} seeds. L. C. Tran provided technical support.

Supporting Online Material

www.sciencemag.org/cgi/content/full/1109977/DC1
Materials and Methods
Figs. S1 and S2
Table S1
References and Notes

19 January 2005; accepted 9 June 2005
Published online 23 June 2005;
10.1126/science.1109977
Include this information when citing this paper.

Supporting Online Material

Materials and Methods

Plant Cultivation, Transformation, Ecotypes and Mutants. Plants were grown on a mixture of Promix (Premier Horticulture, Red Hill, PA), sand, and vermiculite in a 4:2:1 ratio, respectively. Plants were grown in growth chambers with 60% constant relative humidity under 9 hours light at 24°C and 15 hours dark at 20°C. *Agrobacterium* (strain GV3101) transformations and Basta (glufosinate-ammonium) selection of plants expressing the BAR gene for resistance were performed as previously described (*1, 2*).

For Figures 1A-C, 2, and 3A-B,D,F-G we presented data for *rar1-21* (*3*) and *sgt1b*$^{edm1-1}$ (*4*) in the Col-0 ecotype. *sgt1b*$^{edm1-1}$ is defined as a 7 gene deletion that includes *SGT1b* and *rar1-21* is a stop mutation in the CHORD I domain that may still make a truncated protein (*5*). To demonstrate that our findings were not allele specific, we confirmed several mutant phenotypes using alternative *rar1* and *sgt1b* alleles. Loss of *RPS5*-mediated HR in *sgt1b*$^{edm1-1}$ was also observed in *sgt1b*^{eta3} (a 1-bp deletion leading to premature truncation in Col-0, (*6*), Supp. Figure 1A). La-er (*RPP8*) *rar1-10* plants also display a light susceptibility to *Pp* Emco5 that is suppressed in La-er *rar1-10 sgt1b-1* (a 5 bp deletion and a single nucleotide substitution, respectively, resulting in premature stop codons in both cases, (*3, 7*); Supp. Table 1). *RPS5* loss of function in *rar1-20*, a *RAR1* deletion allele, is also restored in *rar1-20 sgt1b*$^{edm1-1}$ (data not shown). Because La-er does not have *RPS5* (*8*), we performed the transgenic RPS5:HA quantification

(Figures 3C,E) with the La-er alleles *rar1-10* and *sgt1b-1*. We obtained similar results for RPS5:HA accumulation using Col-0 (*RPS5*) *rar1-21* and *sgt1b*$^{edm1-1}$ (data not shown).

To confirm enhanced susceptibility to *Pseudomonas syringae* (*Pto*) DC3000 carrying an empty vector (EV) in *rar1-21* (Figure 1B, top panel), we tested *rar1-1*, *rar1-10*, and *rar1-20* in the ecotypes Ws-0, La-er, and Col-0, respectively (Figure 1D). As controls for enhanced disease susceptibility, we used the *eds1-1* (Ws-0) and *eds1-2* (La-er) mutants (*9*). The *rar1 sgt1a* double mutant in Figure 1 was generated with *rar1-21* and *sgt1aKO* (T-DNA insertion) alleles (courtesy of David Hubert, JLD). Genetic markers for genotyping *rar1-20*, *rar1-21*, *sgt1aKO*, *sgt1b*^{edm1}, and *rps5-2* (Col-0 allele used for *rps5*) are available upon request. Using TAIL PCR (*10*), the *RPP8* transgene insertion was mapped to an intergenic region of Chromosome IV, between the loci At4g33460 and At4g33470 at ~nucleotide position 16101504 (TAIR Database; www.*Arabidopsis*.org).

Pathogen Strains and Isolates. For Figure 1A-D and Supplemental Figure 1A, *Pto* DC3000(EV) or *Pto* DC3000(*AvrPphB*) (to trigger *RPS5*) or *Pto* DC3000(*avrRpm1*) (to trigger *RPM1*) or *Pto* DC3000(*avrRpt2*) (to trigger *RPS2*, data not shown) were resuspended in 10mM $MgCl_2$ to ~1X10^5 cfu/mL and syringe infiltrated into leaves of ~4 week old wild type and mutant plants (*11*). Bacterial growth assays were performed as previously described (*11*). The HR tests in Figure 1C and Supplemental Figure 1A were performed identically except the inoculum concentration was raised to 1X10^8 cfu/mL.

The RPM1 HR was assessed 5 hours post inoculation, all other HR phenotypes were examined at ~20 hours post inoculation.

Peronospora parasitica (*Pp*) propagation and inoculation was performed as previously described (*12*). The *Pp* isolates Emco5, Emwa1, Noco2, and Cala1 were maintained on the susceptible *Arabidopsis* ecotypes Col-0, Ws-0, Col-0, and La-er, respectively. The susceptible ecotypes were as follows: The susceptible ecotypes were as follows: Supplemental Figure 1B-D - Ws-0 (*rpp4*; (*13*)); Supplemental Figure 1E, Ws-0 (*rpp31*; (*14*)). Figures 2A-B - Col-0 (*rpp8*; (*15*)); Supplemental Figure 2A - Col-0 (*rpp5*; (*16*)); Supplemental Figure 2B - La-er (*rpp1a*, *rpp2a*, *rpp2b*; (*17, 18*)); The resistant plant lines were as follows: Supplemental Figure 1B-D - Col-0 (*RPP4*); Supplemental Figure 1E - Col-0 (*RPP31*); Figure 2A-B - Col-0 transgenic for *RPP8*; Supplemental Figure 2A - La-er (*RPP5*); Supplemental Figure 2B - Col-0 (*RPP2A/B*).

Trypan blue staining for cell death and the *Pp* structures was performed as previously described (*19*). Pictures of trypan blue stained leaves following Pseudomonas inoculations were done on a standard computer scanner. *Pp* inoculated, trypan blue stained leaves were visualized by light microscope (Nikon Eclipse, Melville, NY).

Geldanamycin (GDA) Experiments. Accumulation of RPM1:Myc, RPS2:HA, and RPS5:HA were examined by protein blot analysis following 10µM GDA (A.G. Scientific, San Diego, CA) infiltration into leaves as described (*20*). We observed similar results 18 and 24 hours post GDA infiltration or when infiltrating 25µM GDA for RPM1:Myc, and

RPS5:HA. We did not observe reductions in RPS2 accumulation following GDA treatment (data not shown) at 10µM, 25µM, or 50µM concentrations over this time course. To test the disease resistance functions of *RPS2*, *RPS5*, and *RPM1*, we performed several independent *in planta* bacterial growth assays by co-inoculating bacteria and GDA as described (*20*). GDA treatment did not diminish disease resistance in any case (data not shown). We often found that GDA treatment resulted in slightly lower pathogen growth on susceptible plants when compared to DMSO (carrier) treated control plants. Furthermore, GDA treated leaves exhibited visually obvious phytotoxic symptoms (yellowing/chlorosis) 48-72 hours post inoculation, independent of bacterial inoculation. This is problematic because 72 hours post-inoculation is the time point when alterations in RPM1 and RPS5 functions are most readily quantifiable. Our findings are inconsistent with previous demonstration of moderate GDA effects on *RPS2* function (*20*). Pleiotropic outcomes from HSP90 manipulation are documented (*21*) and the effects of GDA might be variable depending on specific environmental conditions. While GDA may give minor differences in bacterial growth under specific environmental conditions, this inhibitor serves limited utility. Because plant HSP90 isoforms likely have overlapping functions (*5*), these assays will benefit greatly from the future development of inducible silencing and/or isoform specific dominant negative constructs.

Yeast Two-Hybrid Methods and DNA Manipulations. Directed interaction experiments were performed in the yeast strain EGY48 as previously described (*22*). The yeast "bait" and "prey" vectors pEG202 and pJG4-5, respectively, were modified for

compatibility with the Gateway™ cloning system (vectors courtesy of Hiro Kaminaka, JLD; Gateway™ protocols available online at www.invitrogen.com; Invitrogen, Carlsbad, CA; vector creation details are available on request). The newly created vectors, pEG202gw and pJG4-5gw, were used as the final destination vectors for cloning the LRR from RPM1, RPS2, and RPS5. Each LRR construct was started 10 amino acids upstream of the presumptive LRR start and ended at the stop codon. The primers used to clone each were as follows: **RPM1** - *RPM1 LRR F*: CAC CAA TGA TGA CAG TGA TGG TGA TGA TGC TGC and *RPM1 LRR R*: CTA AGA TGA GAG GCT CAC ATA GAA AGA GCC; **RPS2** - *RPS2 LRR F*: CAC CGT TGA GCC TAG CAT GGG ACA TAC TGA AGC, *RPS2 LRR R*: TCA ATT TGG AAC AAA GCG CGG TAA ATA AC; **RPS5** - *RPS5 LRR F*: CAC CGC TGG TGT TGG GTT ACG TGA AGT ACC AAA, and *RPS5 LRR R*: TTA TGT TTC TCT CCA CCG CCA CCT GGA TG. CACC was added to the forward (F) primer from each pair to facilitate cloning into the Gateway™ entry vector pENTR™/D-TOPO. Each clone was confirmed correct by sequencing and comparison to the TAIR Database. LR Clonase™ enzyme (Invitrogen) was then used to move each clone from pENTR™/D-TOPO to pEG202gw or pJG4-5gw. For the interaction tests, the RPM1, RPS2, and RPS5 LRRs were in pEG202gw. SGT1a and SGT1b were in pJG4-5gw (courtesy David Hubert, JLD). The cloned LRRs from MLA1 and MLA6 (in pEG202) were used for positive and negative SGT1a/b interaction controls, respectively (courtesy Qian-Hua Shen and Paul Shultze-Lefert). As expected, only MLA1 interacted with SGT1a and SGT1b (*22*). Because no interaction was detected between the LRRs from RPM1, RPS2, or RPS5 with either SGT1a or SGT1b, we confirmed that the proteins

were being made in yeast at comparable levels to both MLA1 and MLA6 (see Protein Manipulations).

The following primers were used to clone *RPS5* into pDONOR207 (Invitrogen): *B1Half-RPS5Prom*: CAA AAA AGC AGG CTG GAG CCC CAT GAC CCA AAA AAT GGG, *B2Half-RPS5Stop*: GAA AGC TGG GTC TGT TTC TCT CCA CCG CCA CCT G, *B1 Full Site*: GGG GAC AAG TTT GTA CAA AAA AGC AGG CTT C, and *B2 Full Site*: AGA TTG GGG ACC ACT TTG TAC AAG AAA GCT GGG TC. To facilitate the BP Clonase™ reaction (Invitrogen, Gateway™) required to clone *RPS5* into pDONOR207 (courtesy of Ian Small, URGV INRA, France), a two step PCR reaction was performed. In step one the *RPS5* target was amplified with a portion of the B1 and B2 sites (B1/2 Half primers above), and in step two the B sites were completed with the B1/2 Full Site primers. The final clone has 1,405 bp of *RPS5* native promoter and the full *RPS5* coding sequence (sequence corresponds to *Arabidopsis* AGI nucleotide positions 4143604 to 4147675 on Chromosome I). Sequencing of the entire *RPS5* genomic clone revealed a single silent nucleotide difference in the coding region compared to the TAIR Database. pDONOR207/*RPS5* was then combined with pGWB-BAR (Vector modified from pGWB-14 (kindly provided by T. Nakagawa, Shimane University, Izumo, Japan) and pBAR1 (*12*) to provide *in planta* Basta selection; courtesy Hiro Kaminaka, BFH, JLD) in an LR Clonase™ reaction to create the binary vector pGWB-BAR/*RPS5:HA*. This vector contains three consecutive HA epitopes in the correct translational frame at the C-terminus of the construct. The final destination vector. pGWB-BAR/*RPS5:HA*, was

electroporated into the *Agrobacterium* strain GV3101 for transformation of appropriate plant lines. Transformed plants were subsequently selected by Basta application.

Protein Manipulations. For the fractionation experiments (Figure 3A), tissue samples were taken from multiple independent, first generation plants transformed with pGWB-BAR/*RPS5:HA*. Samples from 10-15 plants were combined and protein was extracted and separated into total, soluble, and membrane fractions by centrifugation in a sucrose buffer (20mM Tris, pH 8.0, 0.33M Sucrose, 1mM EDTA, pH 8.0, 5µM DTT, 1X Sigma Protease Inhibitors (Sigma, St. Louis, MO); (*23*)). Lanes (total, soluble, membrane) were loaded in 1:1:1 cell equivalents corresponding to 50µg of total protein quantified prior to fractionation. No accumulation of RPS5:HA was observed in the soluble fraction of any genetic background following longer exposures. In additional experiments with La-er(*rps5*) transformants, we observed the same distribution pattern for RPS5:HA (data not shown). Equal loading of protein samples was insured by quantifying each sample with Bio-Rad Laboratories (Hercules, CA) protein quantification buffer and visually confirmed by Ponceau Red staining for each nitrocellulose membrane following protein transfer. RPS5:HA was resolved and detected by standard SDS-PAGE protein blotting on a 7.5% gel. Ascorbate peroxidase and RIN4 were resolved on 12% gels. Proteins were transferred to nitrocellulose by standard methods. The ECL Plus Western Blotting Detection System (Amersham Biosciences, Buckinghamshire, England) was used for protein detection for these experiments and all others in this paper. Primary antibody for RPS5:HA - high affinity anti-HA from rat (clone 3F10, Roche Applied Biosciences, Indianapolis, IN); Secondary antibody – anti-Rat from goat conjugated to

horseradish peroxidase (Santa Cruz Biotechnology, Santa Cruz, CA). Proteins were extracted identically in Figure 3C and E, except that they were subjected to a single 3,000 X gravity centrifugation for 5 minutes and the supernatant was quantified for protein concentration. 150µg of total protein for each sample was then subjected to a ~20,000 X gravity centrifugation to concentrate the membrane fraction. This entire membrane pellet was resuspended in 30µL sample buffer and loaded in a SDS-PAGE gel. In Figure 3B, D and G proteins were extracted with standard lysis buffer (50mM Tris, pH 8.0, 1% SDS, 1mM EDTA, 5µM DTT, 1X Sigma Protease Inhibitors). We found that this buffer gave the most consistent extraction of RPM1:Myc and RPS5:HA. 50µg of total protein/lane was loaded. Adobe Photoshop (version 7.0) was used to manipulate all photographic images. In some instances rearrangements of lane order were made, but all photographic adjustments, such as contrast or color, were uniform and performed prior to these rearrangements.

Proteasome Assays. We performed two pharmaceutical assays to examine a role for the proteasome in the reduced RPS5:HA accumulation in *rar1*. In the first, whole leaves from La-er *RPS5:HA* and La-er *rar1-10 RPS5:HA* plants were infiltrated to complete water soaking with the reversible proteasome inhibitor MG132 (100µM from 10mM stock dissolved in DMSO; AG Scientific, San Diego, CA) or DMSO alone. Tissues samples were collected at 0, 2, 4, 6, 8, and 24 hours post infiltration and examined by protein blot analysis. La-er *rar1-10 RPS5:HA* plants infiltrated with the irreversible proteasome inhibitor lactacystin (20µM from 2mM stock dissolved in DMSO; AG Scientific) were also examined 24 hours post infiltration. No apparent change in

RPS5:HA accumulation, either as hyper-accumulation in *RAR1* leaves or re-accumulation in *rar1-21* was observed (data not shown). In the second, we examined the degradation of RPS5:HA and RPM1:Myc over 4 hours in cell free proteasome degradation assays (protocol courtesy of Frank Harmon and Steve Kay, Scripps Institute; (*24*)). Briefly, total proteins are extracted in a non-denaturing HEPES buffer that is subsequently spiked with ATP to drive rapid degradation of proteasome-degradable proteins. Protein degradation in these cell free extracts can be retarded by the addition of proteasome inhibitors such as MG132 and Lactacystin. RPS5:HA and RPM1:Myc did disappear, usually at ~3 hours post ATP addition, but addition of 100μM MG132 or 20μM to 50μM lactacystin did not reproducibly alter the rate of protein disappearance (data not shown). We note that while these assays appear technically sound (e.g. we are able to inhibit the degradation of several proteasome-dependent proteins in our lab), their resolution might be improved using appropriate transgenic lines and crosses to mutations in the proteasome pathway.

Supplemental Figures

Supplemental Figure 1. SGT1b is required for HR mediated by several disease resistance specificities. (A) Two *Arabidopsis sgt1b* alleles are compromised for the *RPS5*-mediated HR. This experiment was performed as in Figure 1D. *sgt1b*^{edm1} is a complete deletion of *SGT1b* and *sgt1b*^{eta3} is a 1 bp change resulting in a truncated sgt1b protein. **(B-E) The HR-promoting function of *SGT1b* in resistance to *Peronospora parasitica* can be *RAR1*-independent.** *RPP4* activates relatively weak disease resistance against *Pp* Emwa1 in cotyledons, **(B-C)**, but is strong in adult leaves **(D)**. Both of these resistance phenotypes were nearly abolished in *rar1*, while *sgt1b* plants exhibited modest levels of sporulation and distinctive trailing necrosis phenotypes. Trailing necroses are thought to result from delayed or weakened HR (*3, 12*). *RPP4* and *RPP31* functions in *rar1 sgt1b* were phenotypically identical to *sgt1b* single mutants. **(B-C)** These experiments were performed on cotyledons as described in Figure 2 A-B, except the *Pp* isolate Emwa1 (*13*) was used to probe *RPP4* function. Double mutant *rar1 sgt1b* plants were indistinguishable from *sgt1b* single mutants in both infected cotyledons and infected adult leaves. In particular, *rar1 sgt1b* plants retained trailing necrosis phenotypes. Representative trypan blue stained leaves are shown **(B, D)**. **(E)** Col-0(*rpp8*) plants are susceptible to *Pp* isolate Emco5 as cotyledons. Adult leaves (fourth pair and beyond) are generally fully resistant. The presumed *R* gene(s) necessary for this resistance has been designated *RPP31* (John McDowell, pers. comm.). Note that the numerous densely stained structures in the first and third panels (Ws-0 ecotype that does not exhibit adult resistance and Col-0 *rar1*,

respectively) are P. parasitica sexual reproductive structures called oospores (*not* HR sites). Dense accumulations of oospores represent strong disease symptoms and are easily differentiated from HR sites under higher magnification. The smaller, densely stained sites in the second panel (Col-0) are typical HR sites.

Supplemental Figure 2. *Peronospora parasitica* resistance specificities are variably impaired in *rar1*, *sgt1b*, and *rar1 sgt1b*. (A-B) These experiments were performed on cotyledons as described in Figure 2A-B, except the *Pp* isolates Noco1 (*13*) and Cala1 (*17*) were used to probe *RPP5* **(A)** and RPP2A/B **(B)** functions, respectively. Cala1 resistance in Col-0 is controlled by two R genes (RPP2A and RPP2B), but is represented in the figure as RPP2 for simplicity (*17*).

Supplemental Table 1. Summary of all genotype/pathogen combinations tested in this study. NB-LRR resistance specificities that are impaired in *rar1*, but recovered in *rar1 sgt1* plants are shown in bold. NB-LRR functions that are additively impaired in *rar1 sgt1b* are shown in italics.

Supplemental Literature Cited

1. T. Altman, B. Damm, U. Halfter, L. Willmitzer, P.-C. Morris, in *Methods in Arabidopsis Research,* C. Koncz, N.-H. Chua, J. Schell, Eds. (World Scientific Publishing Co., London, 1992), pp. 310-330.
2. N. Bechtold, J. Ellis, G. Pelletier, *C. R. Acad. Sci., Paris* **316**, 1194 (1993).
3. P. R. Muskett *et al.*, *Plant Cell* **14**, 979 (2002).
4. M. Tör *et al.*, *Plant Cell* **14**, 993 (2002).
5. D. A. Hubert *et al.*, *Embo J* **22**, 5679 (2003).
6. W. M. Gray, P. R. Muskett, H. W. Chuang, J. E. Parker, *Plant Cell* **15**, 1310 (2003).
7. M. J. Austin *et al.*, *Science* **295**, 2077 (2002).
8. M. T. Simonich, R. W. Innes, *Molec. Plant-Microbe Interact.* **8**, 637 (1995).
9. J. E. Parker *et al.*, *Plant Cell* **8**, 2033 (1996).
10. Y. G. Liu, N. Mitsukawa, T. Oosumi, R. F. Whittier, *Plant J* **8**, 457 (1995).
11. J. L. Dangl *et al.*, in *Methods in Arabidopsis Research,* C. Koncz, N.-H. Chua, J. Schell, Eds. (World Scientific, Singapore, 1992), pp. 393-418.
12. B. F. Holt III *et al.*, *Dev Cell* **2**, 807 (2002).
13. E. A. van der Biezen, C. T. Freddie, K. Kahn, J. E. Parker, J. D. Jones, *Plant J* **29**, 439 (2002).
14. M. A. Torres, J. L. Dangl, J. D. G. Jones, *Proc. Natl. Acad. Sci. USA* **99**, 523 (2002).
15. J. M. McDowell *et al.*, *Plant Cell* **10**, 1861 (1998).
16. J. E. Parker *et al.*, *Plant Cell* **9**, 879 (1997).
17. E. Sinapidou *et al.*, *Plant J* **38**, 898 (2004).
18. M. A. Botella *et al.*, *Plant Cell* **10**, 1847 (1998).
19. E. Koch, A. J. Slusarenko, *Plant Cell* **2**, 437 (1990).
20. A. Takahashi, C. Casais, K. Ichimura, K. Shirasu, *Proc Natl Acad Sci U S A* **100**, 11777 (2003).
21. T. A. Sangster, C. Queitsch, *Curr Opin Plant Biol* **8**, 86 (2005).
22. S. Bieri *et al.*, *Plant Cell* **16**, 3480 (2004).
23. D. C. Boyes, J. Nam, J. L. Dangl, *Proc. Natl. Acad. Sci., USA* **95**, 15849 (1998).
24. P. Mas, W. Y. Kim, D. E. Somers, S. A. Kay, *Nature* **426**, 567 (2003).

Supplemental Figure 1

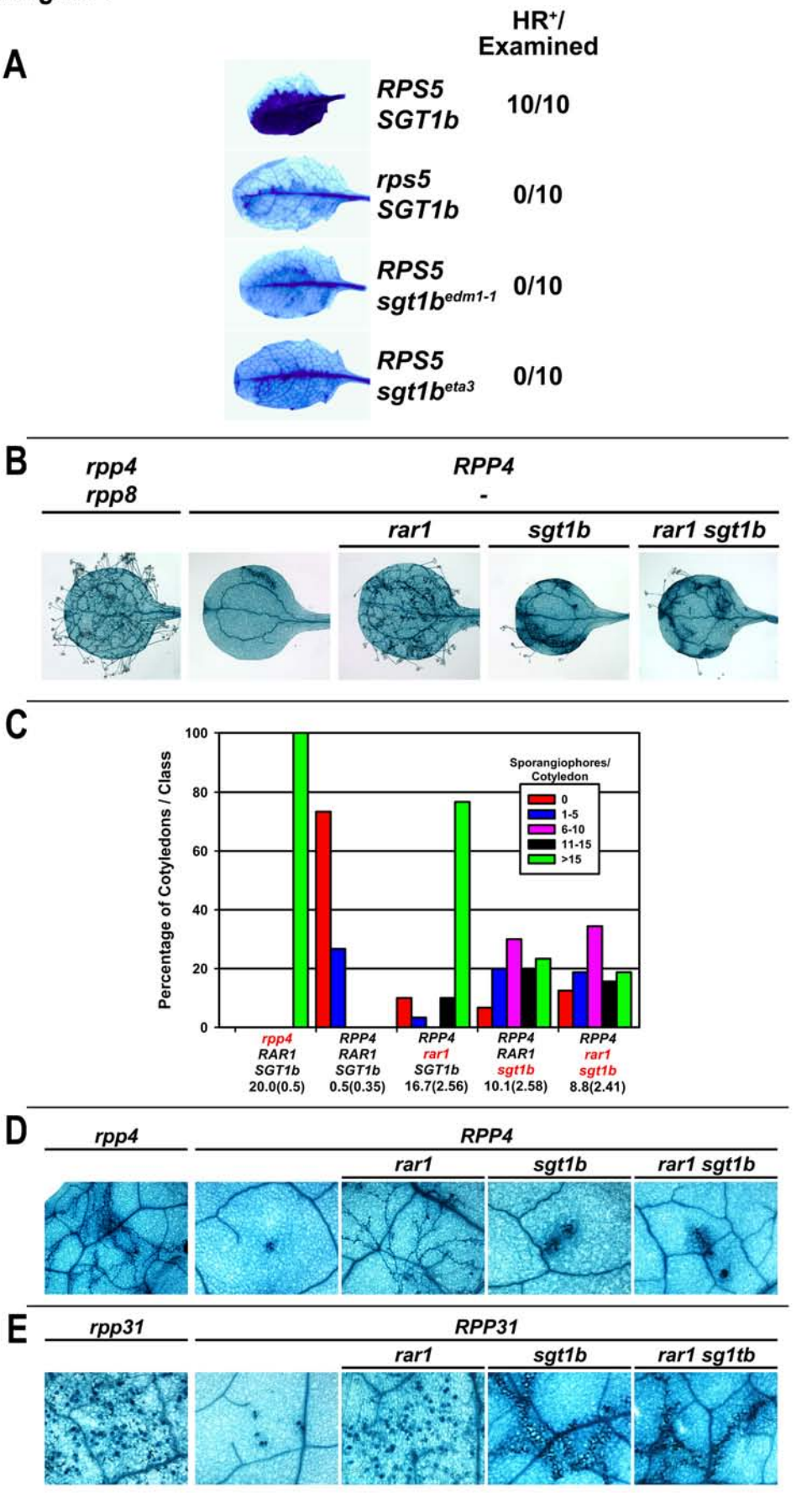

Supplemental Figure 2

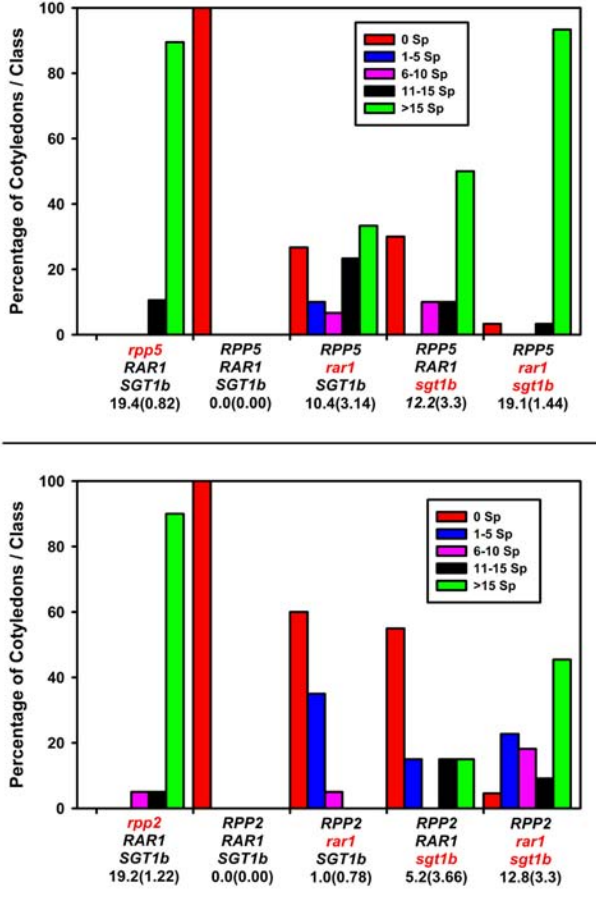

Supplemental Table 1

Pathogen	Isolate or Strain	Ecotype	R Gene	N-Term	*rar1*	*sgt1b*	*rar1/sgt1b*
*P. parasitica**	Cala2	Ws-0	*RPP1A*	TIR	R	R	ND
	Cala2	*Col-0*	*RPP2A/B*	*TIR*	*LS*	*MS*	*HS*
	Emwa1	**Col-0**	***RPP4***	**TIR**	**HS**	**MS**	**MS**
	Emwa1	**Col-0^{Adult}**	***RPP4***	**TIR**	**HS**	**TN**	**TN**
	Noco2	*La-er*	*RPP5*	*TIR*	*MS*	*MS*	*HS*
	Noco2	Col-0	*rpp5***	**-**	S	S(↑V)	S(↑V)
	Hiks1	*Col-0*	*RPP7*	*non-TIR*	*R*	*MS*	*HS*
	Emco5	**La-er**	***RPP8***	**CC**	**LS**	**R**	**R**
	Emco5	**Col-0**	***RPP8^{La-er}***	**CC**	**LS**	**R**	**R**
	Emco5	**Col-0^{Adult}**	**Unknown**	**-**	**HS**	**LS**	**LS**
P syringae pv. *tomato*	AvrRpm1	Col-0	*RPM1*	CC	S	R	S
	AvrRpt2	Col-0	*RPS2*	CC	S	R	S
	AvrRps4	Col-0	*RPS4*	TIR	S	R	S
	AvrPphB	**Col-0**	***RPS5***	**CC**	**S**	**R**	**R**

NOTES:

*Unless otherwise noted, all *Peronospora parasitica* tests were done on 7 day old cotyledons

** = Col-0(*rpp5*) plants were examined for sporangiophore emergence 4 days post inoculation

R = Resistant

TN = Trailing Necrosis

LS = Light Sporulation (<5 Sp/Cot)

MS = Moderate Sporulation (5-12 Sp/Cot)

HS = Heavy Sporulation (>12 Sp/Cot)

S(↑V) = Increased pathogen virulence as measured by rate of sporangiophore emergence

RPP8^{La-er} = Transgene from La-er ecotype expressed behind native promoter

Unknown = The gene(s) conferring *Pp* Emco5 adult resistance is not yet cloned

ND = Not Determined